

# Topological Optimization of Shell Laminate Composites Parts Manufactured by the TFP Process

Peng YU<sup>1,a\*</sup>, Jessy SIMON<sup>2,b</sup>, Christophe BINETRUY<sup>2,c</sup>  
and Nahiene HAMILA<sup>1,d</sup>

<sup>1</sup>IRDL UMR CNRS 6027, Bretagne INP, Brest, F-29200, France

<sup>2</sup>GeM, UMR CNRS 6183, Nantes Université, Ecole Centrale Nantes, Nantes, F-44000, France

<sup>a</sup>peng.yu@enib.fr, <sup>b</sup>jessy.simon@ec-nantes.fr, <sup>c</sup>christophe.binetruy@ec-nantes.fr,

<sup>d</sup>nahiene.hamila@enib.fr

**Keywords:** Topology optimization, TFP process, curvilinear fibers

**Abstract.** While the use of composite materials increases the specific stiffness of structural parts, their manufacture using automated fiber placement processes such as Tailored Fiber Placement (TFP) allows for the addition of functionalization. An example of such a part is the hydrofoil, which can gain hydrodynamic performance if its shape adapts to the different loads encountered in the three modes of navigation. One method that can meet these requirements is passive functionalization. In this context, the development of digital design support tools is essential. Among them, topology optimization is a well-established method. This work focuses on the development of a strategy for optimizing the topology or the fiber density distribution of the part and the orientation of the fibers for composite materials with an objective function of path generating type allowing passive functionalization. A method for generating fiber trajectories for the TFP process is also presented. The topology optimization results of a cantilever type test case and a shell plate are shown and discussed.

## Introduction

Topology optimization is one of the most advanced structural design methods, aiming to automatically find the optimal structure within the design domain based on loads, given constraints, and an objective function to be satisfied. In a topology optimization problem for a mechanical part, satisfying the objective involves determining the material arrangement within the design space. It can be defined as a binary problem consisting of finding the distribution of void or filled areas that minimizes the work done by external forces or compliance subjected to a volume constraint [1]. Some other problems with different objectives functions and constraint can also be solved. For instance, finding the lightest structure which meets a specific failure criterion [1]. Numerical methods for topological optimization have been extensively studied, notably by Bendsøe [2] who introduced a homogenization approach [3], but also the density-based method with the SIMP (Solid Isotropic Material with Penalization) scheme [1, 4] and level-set-based topological optimization [5, 6].

The TFP (Tailored Fiber Placement) process is a relatively new automated textile process for producing composites reinforcements with curvilinear fiber paths [7]. When combined with the forming process of continuous fiber-reinforced composite materials, the TFP process offers a high degree of design freedom by allowing the fibers to be arranged in an optimal manner. The principle of TFP is illustrated in Fig. 1. The embroidery head fixes a continuous tow of fiber to a flat backing material by creating a zigzag stitch. The TFP has demonstrated significant potential for application in the manufacture of small and medium-sized lightweight composite structures in the aerospace, automotive, and energy industries [8, 9, 10].

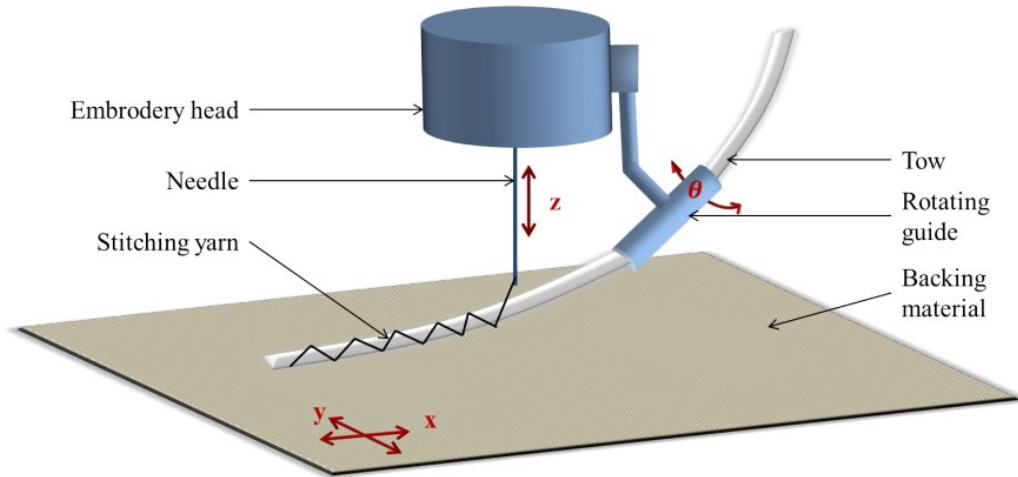


**Fig. 1** Schematic representation of the TFP principle [11]

For the TFP process, the most important factor is determining the fiber deposition path, which will significantly influence the mechanical performance of the composite part. In the article by Papapetrou et al. [12], three different methods were applied and compared to generate and optimize the fiber path. The first is the offset method, which creates contours parallel to the boundary of the solid domain at equal intervals until they intersect or encounter void. This method, while applicable to very complex geometries, can introduce abrupt changes along the paths. The second is called the EQS method, it uniformly distributes a constant number of points along each cross-section of the optimized solid area, and then these points are connected in the span direction. Finally, the third is the streamline method, which will be explained with more details in the Methods section.

The energy method [12] is commonly employed to enhance the smoothness and continuity of fiber paths, where fiber orientations are determined by minimizing the strain or stress energy. Gea and Luo [13] investigated this method and demonstrated that the resulting orientations generally align with the principal stress or strain directions for materials that are orthotropic with relatively weak shear coupling, as well as for certain strongly coupled materials under shear.

## Methods

**Material model.** The orthotropic material model with variable fiber volume fraction  $v_f$  [14] is used in this work. The following micromechanical models are used to determine the effective properties of the composite as function of  $v_f$ :

$$E_1 = v_f E_f + (1 - v_f) E_m, \quad (1)$$

$$E_2 = \frac{E_f E_m}{v_f E_m + (1 - v_f) E_f}, \quad (2)$$

$$G_{12} = \frac{G_f G_m}{v_f G_m + (1 - v_f) G_f}, \quad (3)$$

$$v_{12} = v_f v_f + (1 - v_f) v_m. \quad (4)$$

where  $E_1$  is Young's modulus along axis 1,  $E_2$  is Young's modulus along axis 2,  $v_{12}$  is Poisson's ratio,  $G_{12}$  is in-plane shear modulus.  $E_f$ ,  $G_f$ ,  $v_f$  represent Young's modulus, in-plane shear modulus and Poisson's ratio of the fiber material, respectively, and  $E_m$ ,  $G_m$ ,  $v_m$  represent Young's modulus, in-plane shear modulus and Poisson's ratio of the matrix material, respectively. The axis 1 is determined by fiber orientation  $\theta$  and the axes 2 and 3 are taken to be orthogonal to axis 1.

In numerical computation, the  $v_f$  of each element is obtained by a continuous design variable fiber density  $\rho_f$  by following equation:

$$v_f^i = (1 - \rho_f^i)v_{f,min} + \rho_f^i v_{f,max}. \quad (5)$$

where  $v_{f,min}$  and  $v_{f,max}$  represent the minimum and maximum local fiber volume fraction, the intermediate values of  $v_f$  can thus be determined through linear interpolation.

The 2D orthotropic stiffness tensor  $\mathbf{C}$  is defined as follows:

$$\mathbf{C} = \begin{bmatrix} \frac{E_1}{1-\nu_{12}\nu_{21}} & \frac{\nu_{12}E_2}{1-\nu_{12}\nu_{21}} & 0 \\ \frac{\nu_{21}E_1}{1-\nu_{12}\nu_{21}} & \frac{E_2}{1-\nu_{12}\nu_{21}} & 0 \\ 0 & 0 & G_{12} \end{bmatrix} \quad (6)$$

The fiber orientation  $\theta$  is considered through transformation matrix  $\mathbf{T}$ :

$$\mathbf{T} = \begin{bmatrix} \cos^2 \theta & \sin^2 \theta & 2 \sin \theta \cos \theta \\ \sin^2 \theta & \cos^2 \theta & -2 \sin \theta \cos \theta \\ -\sin \theta \cos \theta & \sin \theta \cos \theta & \cos^2 \theta - \sin^2 \theta \end{bmatrix} \quad (7)$$

For 3D shell element, the reduced constitutive tensor and SB8 solid-shell element from the work of M. Dia [15] are applied in order to model correctly shell elements behavior. It easier to implement the cinematics of SB8 element since it's based only on displacements. Quadrangle-type elements will be used for 2D calculations and the 3D solid-shell elements will be used for a laminate subjected to out-of-plane forces.

**Topology optimization: Density-based method.** The density-based method is a classic topological optimization method [1]. Depending on the type of material, the method scheme may differ, for example, SIMP for isotropic materials and SOMP (Solid Orthotropic Material With penalization). In this method, a density  $\rho$  between 0 and 1 is assigned to each element to represent its state: density 0 corresponds to the void and density 1 to the solid. Intermediate densities are obtained by interpolation. Thus, a discretized binary problem is converted into a continuous problem.

The minimization of compliance topology optimization problem with SOMP scheme can be formulated as follows:

$$\begin{aligned} & \text{find } \rho = [\rho_1, \rho_2, \dots, \rho_n]^T, \theta = [\theta_1, \theta_2, \dots, \theta_n]^T \\ & \text{minimize } c(\rho_{phys}, \theta) = \mathbf{f}^T \mathbf{u}(\rho_{phys}, \theta) \\ & \text{subjected to } V(\rho_{phys}) = \rho_{phys}^T \mathbf{V} - V_{lim} \leq 0 \\ & \rho \in x, x = [\rho \in \mathbb{R}^n: 0 \leq \rho \leq 1] \end{aligned} \quad (8)$$

where  $\rho$  is the element density,  $\rho_{phys}$  is the filtered density,  $\theta$  is the fiber orientation,  $n$  is the number of elements,  $c$  is the compliance,  $\mathbf{f}$  is the force vector,  $\mathbf{u}$  is the displacement vector,  $\mathbf{V}$  is a vector containing the volumes of all elements and  $V_{lim}$  is the prescribed threshold of volume of the final structure.

Besides minimization of compliance, the path generating problem is also studied in this paper. This type of problem aims to achieve a target displacement at specified locations so the objective function can be written as the sum of the error between the actual displacement and the target displacement at the target locations in least squares form.

$$\begin{aligned} & \text{find } \rho_f = [\rho_{f1}, \rho_{f2}, \dots, \rho_{fn}]^T, \theta = [\theta_1, \theta_2, \dots, \theta_n]^T \\ & \text{minimize } \varepsilon(\rho_f, \theta) = \frac{1}{2} (\mathbf{u} - \mathbf{u}_{target})^T \mathbf{D} (\mathbf{u} - \mathbf{u}_{target}) \\ & \text{subjected to } \mathbf{K}(\rho_f) \mathbf{u}(\rho_f) = \mathbf{f} \\ & \rho_f \in x, x = [\rho_f \in \mathbb{R}^n: 0 \leq \rho_f \leq 1] \end{aligned} \quad (9)$$

where  $\rho_f$  is the fiber density,  $\theta$  is the fiber orientation,  $n$  is the number of elements,  $\varepsilon$  is the error,  $\mathbf{u}$  is the displacement vector,  $\mathbf{u}_{target}$  is the target displacement vector that only has prescribed values on the target degrees of freedom, the matrix  $\mathbf{D}$  is a diagonal matrix where all elements on the diagonal are 0 except for the degree of freedoms representing the target displacement,  $\mathbf{K}$  is the global stiffness matrix and  $\mathbf{f}$  is the force vector.

In the first formulation, the aim is to minimize the compliance with a constraint of the total volume and fiber orientation, therefore the density of element and the fiber orientation are chosen as design variables. In the second formulation, we are interested in a target deformation and we only manipulate the fiber volume fraction and the orientation, no material will be removed. In engineering application, there is also no reason to remove some elements and leave a hole when we want to fabricate a composite plate. Based on this context, unlike Eq. 8, the total volume constraint is removed from Eq. 9 and we choose fiber density and orientation as design variables to solve path generating problem.

**Fiber path generation: Streamline method.** Since the orientation field  $\theta$  is a discrete solution to the optimization problem, manufacturable continuous fiber paths with the TFP process must be determined. For this, the streamline method is used. This method calculates a function  $\psi$  whose gradient is orthogonal to the fiber orientations  $\theta$ . Thus, if  $\psi$  is calculated on a mesh, a scalar field of  $\Psi$  is obtained, allowing the generation of continuous trajectories by drawing level-sets from the values of  $\Psi$ . These level-sets represent the fiber paths. A smoothing method for the change in orientation between neighboring elements is also applied to obtain a more continuous and smoother trajectory.

The streamlines are therefore calculated using the following minimization scheme:

$$\begin{aligned} \min_{\psi} \mathbf{I}(\psi) &= \frac{1}{2} \int \alpha_1(x) \cdot |\nabla\psi - k\mathbf{V}_{\perp}|^2 d\Omega \\ \text{where: } \alpha_1(x) &= 0, \text{ if } x \in \Omega_{void} \\ \alpha_1(x) &= 1, \text{ if } x \in \Omega_{solid} \end{aligned} \quad (10)$$

where  $k$  is a coefficient that allows control of the spacing between the tow of fibers and  $\mathbf{V}_{\perp}$  is the vector perpendicular to the fibers directly obtained from the fiber angle  $\theta$ .

## Results and Discussions

In this section, two numerical tests are conducted to evaluate the performance of the proposed method. For the first formulation, a test from the work of Papapetrou et al. [12] is reproduced to validate the topology optimization method, then the proposed fiber path generation approach is also tested. For the second formulation, a simple shell plate is tested, which necessitates the integration of shell-like element such as SB8. In this test, we want to assess how the fiber density distribution and fiber orientation will influence the final fiber paths, therefore such a flexion plate with fiber density initially uniform everywhere and aligned with X direction is chosen.

**Case 1: cantilever2D.** The topology optimization with the first formulation (Eq. 8) is carried out on a 2D cantilever model as shown in Fig. 2. The design domain is a  $200 \times 100$  rectangle. Four-nodes quad elements of dimension  $2 \times 2$  is used. The left side of domain is clamped and a concentrated force of  $1 \times 10^5$  N is applied at the middle of the right edge of design domain.

As for the properties of material, in Eq. 8 there is no fiber volume fraction, so it is considered that the fiber density  $\rho_f$  in Eq. 5 is 1 everywhere in the material model. Other properties are taken from the paper of Papapetrou et al. [12]:  $E_1$  is 80 GPa,  $E_2$  is 35 GPa,  $G_{12}$  is 30.1 GPa and  $\nu_{12}$  is 0.33. It is noticed that the properties adopted here do not correspond to a specific industrial composite material, but are introduced for numerical validation of our model.

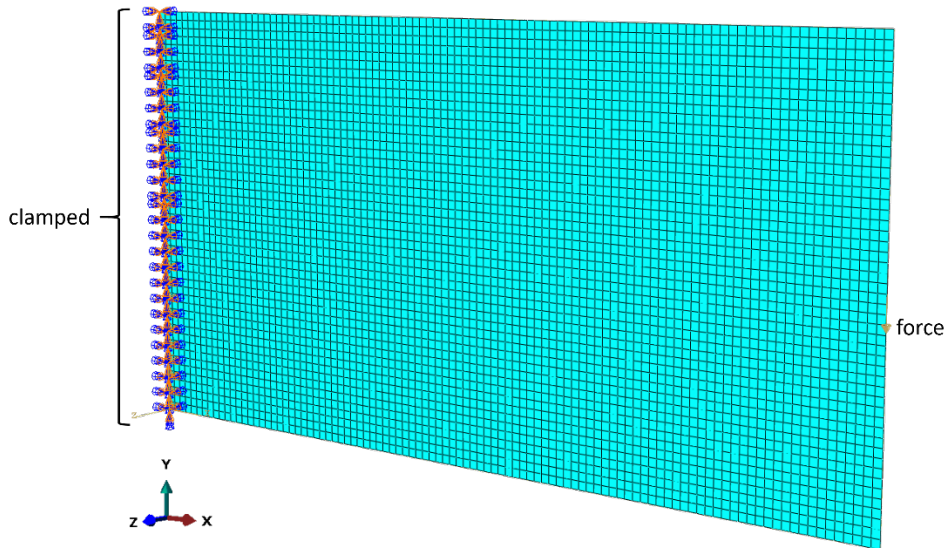


**Fig. 2** Mesh, boundary conditions and loads of case 1: cantilever2D

Fig. 3 shows the results of topology optimization of case 1. In the results, the elements having a density  $\rho$  smaller than 0.5 are considered as void so removed. The red arrows represent the fiber orientation, which is first aligned with the first principal direction of each element, then averaged by a filter within a certain range with their neighbor elements. The orientations are averaged and smoothed in the purpose of generating a smooth and continuous fiber trajectory, avoiding sudden change of direction, which is not suitable in TFP process. The yellow lines represent the fiber paths generated based on the fiber orientation, it can be seen that with a symmetric fiber orientations field, we obtain smooth and symmetric fiber paths, they tend to converge at the point where the load is applied.

It should be noticed that the fiber paths near the boundary are sometimes disconnected. This is for the reason of stair-like boundaries. In the future study, the mesh will be refined and some smoothen algorithm will be applied to have more continuous paths on the boundaries.

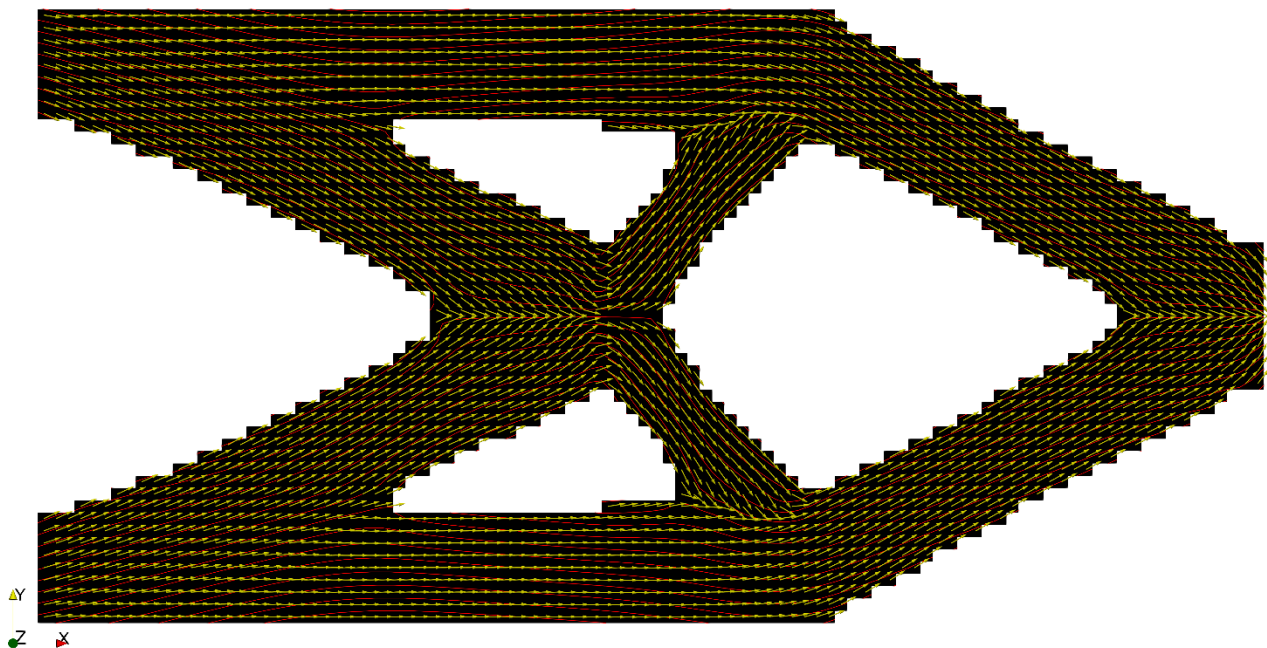


**Fig. 3** Results of case 1: topology (black), fiber orientation (yellow) and fiber paths (red)

**Case 2: flexion plate.** A path generating problem with the second formulation (Eq. 9) is studied on a 1-layer 3D flexion shell plate model as shown in Fig. 4. The design domain is a  $200 \times 100$  rectangle with layer thickness of 0.2. Solid-shell SB8 elements of dimension  $2 \times 2 \times 0.2$  is used. The

left end surface of domain is clamped and a uniform distributed force of 10 N is applied on the right end surface of design domain.

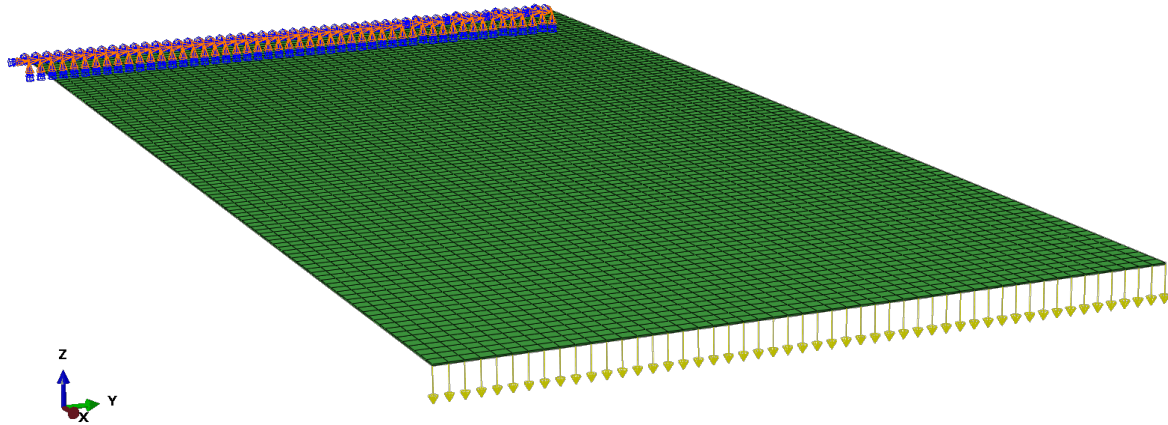


**Fig. 4** Mesh, boundary conditions and loads of case 2: flexion plate

Material properties are set as follows [14]:  $E_f$  is 110 GPa,  $E_m$  is 2.3 GPa,  $G_f$  is 6.2 GPa,  $G_m$  is 1.5 GPa and  $\nu_f$  and  $\nu_m$  are 0.31. The maximum and minimum local fiber volume fraction are 0.6 and 0.2, respectively. The target displacements set on the right end surface to the negative Z direction with the magnitude of 2.5 while the theoretic mechanical solution of the displacement on the right end is between 1.18 and 3.32, which corresponds to maximum and minimum fiber volume everywhere with fiber aligned with the x-axis, respectively.

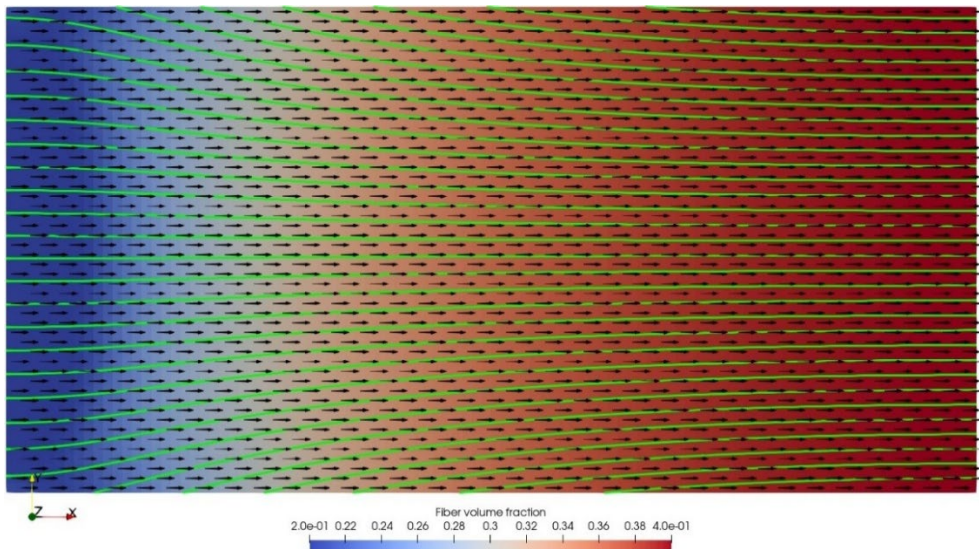


**Fig. 5** Results of case 2: distribution of  $\nu_f$ , fiber orientation (black) and fiber paths (green)

Fig. 5 shows the results of topology optimization of case 2. The black arrows represent the fiber orientation and the green lines represent the fiber paths generated based on the fiber orientation. The fiber volume fractions are in the range of 0.2 to 0.4. Extracting the results from the first iteration, it can be known that the fiber density is still almost uniform in 0.5 (initialized value), the fibers are all aligned with the x-axis and the generated fiber paths are almost parallel lines. The Z component of displacement of the right end is about -1.7, this means the plate is too rigid to achieve the target displacement at the start. Based on this situation, it can be seen that, in order to achieve the target uniform displacements, the fiber volume fraction of the whole plate is not homogeneous but has a gradient from left end to right end. On the left end, the fiber volume fraction is almost the minimum, it decreased a lot compared with the first iteration to make the plate more flexible, so the fiber paths are less densified. Along the X direction, the fiber volume fraction increases so the distance between adjacent fiber paths becomes smaller. On the right end of the plate, the fiber paths are much more densified that on the left end. Furthermore, it can be seen that the fiber orientations do not change much and remains aligned with X direction, while the fiber paths on the left end are not exactly

aligned with the fiber orientations since they are influenced by a lower fiber volume fraction, which seems consistent. By checking the sensibility of the objective function with respect to the orientation, it can be found that the sensibility of orientation is almost zero in this case, that's why only the fiber volume fraction changed over iterations.

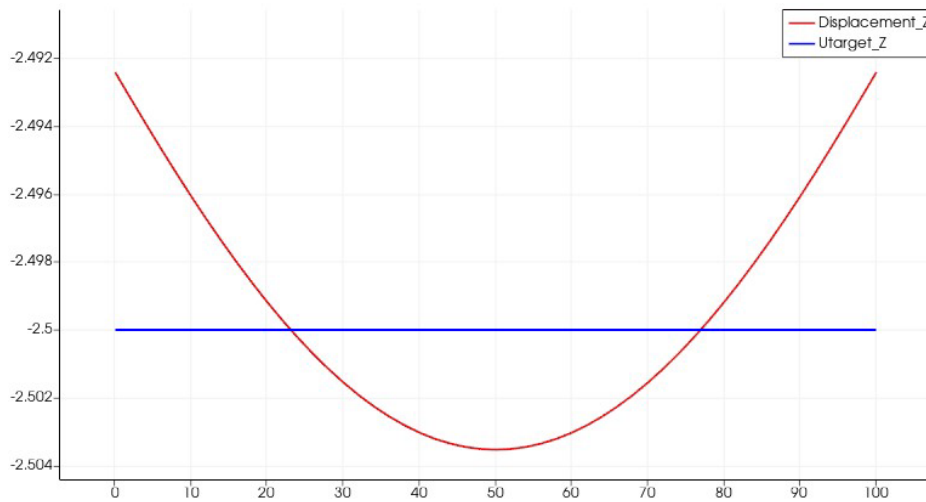


**Fig. 6** Result of case 2: displacement on the right end surface along the width direction

In Fig. 6, the red curve shows the Z component of displacement at the middle of the right end surface along the width direction and the blue line represents the target displacement. The final objective function is  $6.368e-4$ . It can be seen that, the results are varied from -2.4925 to -2.5035, very close to the target displacements value -2.5. It is also interesting to observe that, even though the results are very close to the target, they are not uniform but change in a quadratic form along the width direction, which is expected for a plate under bending.

## Conclusion

This work focuses on the design of composite parts, especially shell plate with target displacement, through topology and material optimization. Unlike previous works, the volume constraint on density or fiber density is removed from the formulation of path generating problem, which makes the problem more relevant to engineering practice. The presented method for generating continuous fiber paths from a discrete vector field resulting from the optimization of the topology and fiber orientation will be used to manufacture parts using the TFP process and experimental testing will be conducted to validate the optimized design.

## Acknowledgements

The authors acknowledge financial support from Bretagne region and Carnots ARTS project.

## References

- [1] M.P. Bendsoe, O. Sigmund, *Topology optimization: theory, methods, and applications*, Springer Science & Business Media, 2013.
- [2] M.P. Bendsøe and N. Kikuchi, "Generating optimal topologies in structural design using a homogenization method," *Computer Methods in Applied Mechanics and Engineering*, vol. 71, no. 2, pp. 197–224, Nov. 1988, doi: [https://doi.org/10.1016/0045-7825\(88\)90086-2](https://doi.org/10.1016/0045-7825(88)90086-2).
- [3] Y. Wang, X. Li, K. Long, and P. Wei, "Open-Source Codes of Topology Optimization: A Summary for Beginners to Start Their Research," *Computer Modeling in Engineering & Sciences*, vol. 137, no. 1, pp.1-34, Jan. 2023, doi: <https://doi.org/10.32604/cmescs.2023.027603>.

- 
- [4] M.P. Bendsøe, “Optimal shape design as a material distribution problem,” *Structural Optimization*, vol. 1, no. 4, pp. 193–202, Dec. 1989, doi: <https://doi.org/10.1007/bf01650949>.
- [5] M. Y. Wang, X. Wang, and D. Guo, “A level set method for structural topology optimization,” *Computer Methods in Applied Mechanics and Engineering*, vol. 192, no. 1–2, pp. 227–246, Jan. 2003, doi: [https://doi.org/10.1016/s0045-7825\(02\)00559-5](https://doi.org/10.1016/s0045-7825(02)00559-5).
- [6] G. Allaire, F. Jouve, and A.-M. Toader, “Structural optimization using sensitivity analysis and a level-set method,” *Journal of Computational Physics*, vol. 194, no. 1, pp. 363–393, Feb. 2004, doi: <https://doi.org/10.1016/j.jcp.2003.09.032>.
- [7] P. Mattheij, K. Gliesche, and D. Feltin, “Tailored Fiber Placement-Mechanical Properties and Applications,” *Journal of Reinforced Plastics and Composites*, vol. 17, no. 9, pp. 774–786, Jun. 1998, doi: <https://doi.org/10.1177/073168449801700901>.
- [8] Axel Spickenheuer, M. Schulz, Konrad Gliesche, and G. Heinrich, “Using tailored fibre placement technology for stress adapted design of composite structures,” *Plastics Rubber and Composites*, vol. 37, no. 5, pp. 227–232, Jun. 2008, doi: <https://doi.org/10.1179/174328908x309448>.
- [9] K. Uhlig, A. Spickenheuer, L. Bittrich, and G. Heinrich, “Development of a Highly Stressed Bladed Rotor Made of a CFRP Using the Tailored Fiber Placement Technology,” *Mechanics of Composite Materials*, vol. 49, no. 2, pp. 201–210, May 2013, doi: <https://doi.org/10.1007/s11029-013-9336-4>.
- [10] H.S. Almeida, Lars Bittrich, T. Nomura, and Axel Spickenheuer, “Cross-section optimization of topologically-optimized variable-axial anisotropic composite structures,” *Composite structures*, vol. 225, pp. 111150–111150, Oct. 2019, doi: <https://doi.org/10.1016/j.compstruct.2019.111150>.
- [11] J. Simon, “Numerical simulation and experimental investigation of the forming of tailored fibre placement preforms: a mixed embedded-ALE finite element formulation,” PhD thesis, École centrales de Nantes, *Cnrs.fr*, Jun. 2022, doi: <https://theses.hal.science/tel-03868340>.
- [12] V.S. Papapetrou, C. Patel, and A.Y. Tamijani, “Stiffness-based optimization framework for the topology and fiber paths of continuous fiber composites,” *Composites Part B: Engineering*, vol. 183, p. 107681, Feb. 2020, doi: <https://doi.org/10.1016/j.compositesb.2019.107681>.
- [13] H. C. Gea and J. H. Luo, “On the stress-based and strain-based methods for predicting optimal orientation of orthotropic materials,” *Structural and Multidisciplinary Optimization*, vol. 26, no. 3–4, pp. 229–234, Feb. 2004, doi: <https://doi.org/10.1007/s00158-003-0348-x>.
- [14] F. Zhang, B. Li, W. Wo, X. Hu, M. Chang, and P. Jin, “Topology Design of 3D Printing Continuous Fiber-Reinforced Structure Considering Strength and Non-Equidistant Fiber,” *Advanced Engineering Materials*, vol. 26, no. 1, Nov. 2023, doi: <https://doi.org/10.1002/adem.202301340>.
- [15] M. Dia, “Hexahedral and prismatic solid-shell for nonlinear analysis of thin and medium-thick structures” PhD thesis, Université de Lyon, *Hal.science*, Jun. 2020, doi: <https://theses.hal.science/tel-03178821>.